PHYSICAL REVIEW D **91,** 114020 (2015)

Glueball physics in QCD

Y. M. Cho,[1,2,3,*] X. Y. Pham,[4] Pengming Zhang,[1,5] Ju-Jun Xie,[1,5] and Li-Ping Zou[1,5,6]

[1]*Institute of Modern Physics, Chinese Academy of Science, Lanzhou 730000, China*
[2]*Administration Building 310-4, Konkuk University, Seoul 143-701, Korea*
[3]*School of Physics and Astronomy, Seoul National University, Seoul 151-747, Korea*
[4]*Lab de Physique Theorique et Hautes Energies Tour 24-25, 1er Etage, 4 Place Jussieu, Universite Paris VI, F-75252 Paris, France*
[5]*State Key Laboratory of Theoretical Physics, Institute of Theoretical Physics, Chinese Academy of Sciences, Beijing 100190, China*
[6]*Institute of Basic Sciences, Konkuk University, Seoul 143-701, Korea*

(Received 30 March 2015; published 12 June 2015)

The Abelian decomposition of QCD which decomposes the gluons to the color neutral binding gluons and the colored valence gluons shows that QCD can be viewed as the restricted QCD (RCD) made of the binding gluons which has the valence gluons as colored source, and simplifies the QCD dynamics greatly. In particular, it tells that the gauge covariant valence gluons can be treated as the constituents of hadrons, and generalizes the quark model to the quark and valence gluon model. So it provides a comprehensive picture of glueballs and their mixing with quarkoniums, and predicts new hybrid hadrons made of quarks and valence gluons. We discuss how these predictions could be confirmed experimentally. In particular we present a systematic search for the ground state glueballs and their mixing with quarkoniums below 2 GeV in 0^{++}, 2^{++}, and 0^{-+} channels within the framework of QCD, and predict the relative branching ratios of the radiative decay of ψ to the physical states.

DOI: 10.1103/PhysRevD.91.114020 PACS numbers: 12.38.-t, 11.15.-q, 11.15.Tk, 12.38.Aw

I. INTRODUCTION

One of the important issues in hadron spectroscopy is the identification of glueballs. The general wisdom is that QCD must have the glueballs made of gluons. In early days the gauge invariant combinations of the QCD field strength were suggested to generate the glueballs [1–3]. Later several models of glueballs including the bag model and the constituent model have been proposed [4–12]. Moreover, the lattice QCD has been able to estimate the mass of the low-lying glueballs [13–16].

But so far the search for the glueballs has not been so successful for two reasons. First, theoretically there has been no consensus on how to construct the glueballs from QCD. For example, there has been the proposal to make the glueballs with "the constituent gluons," but a precise definition of the constituent gluon was lacking [6,7]. This has made it difficult for us to predict what kind of glueballs we can expect.

The other reason is that it is not clear how to identify the glueballs experimentally. This is partly because the glueballs could mix with the quarkoniums, so that we must take care of the possible mixing to identify the glueballs experimentally [6,7]. This is why we have very few candidates of the glueballs so far, compared to huge hadron spectrum made of quarks listed by Particle Data Group (PDG) [17].

This makes the search for the glueballs an important issue in hadron spectroscopy. Indeed, one of the main purposes of the Jefferson Lab 12 GeV upgrading is to search for the glueballs [18]. The purpose of this paper is to provide a comprehensive and clear picture of the glueballs in QCD, to study the possible mixing with the quarkoniums, and to discuss how to identify them theoretically and experimentally.

Actually, it is not difficult to define the gauge covariant colored gluons which form color octet which could be identified as the constituent gluons. This can be done with the Abelian decomposition known as the Cho decomposition or Cho-Duan-Ge (CDG) decomposition, which decomposes the QCD gauge potential to the color neutral restricted potential and the colored valence potential gauge independently [19–23].

What is remarkable about this decomposition is that the restricted potential has the full non-Abelian gauge symmetry and the valence potential transforms gauge covariantly. So we can construct the restricted QCD (RCD) which describes the core dynamics of QCD with the restricted potential, and view QCD as RCD which has the valence gluons as the gauge covariant colored source.

Clearly the Abelian decomposition tells that there are two types of gluons which play different roles. The restricted potential describes the color neutral binding gluons which confines the colored source, and the valence potential describes the colored valence gluons which become the colored source of QCD.

*ymcho7@konkuk.ac.kr

This seems to justify the intuitive idea of the constituent gluons, because the valence gluons can be viewed as the constituents of hadrons. But there is an important difference. Here the binding gluons are not treated as the constituents. To understand this consider the atomic bound states in QED. Obviously we have photons as well as electrons (and protons) in atoms, but only the electron and proton become the constituents because only they determine the atomic structure of the periodic table. The photons play no role in the periodic table. They are there as the electromagnetic field to provide the binding force and binding energy, not as a constituent particle to determine the atomic structure.

Exactly the same way we need quarks and gluons to make the proton. But again the gluons inside the proton does not play any role in the baryon spectrum. This means that they must be the "binding" gluons, not the "constituent" gluons, which (just like the photons in atoms) provide only the binding force and the binding energy of the proton. If so, what are the binding gluons and the constituent gluons? And how can one distinguish them? This is the problem of the constituent model.

Clearly the Abelian decomposition provides a natural answer. It tells that there are indeed two types of gluons, binding gluons and valence gluons, and only the valence gluons can be treated as the constituent gluons. And the gluons in proton are the binding gluons, not the valence gluons, because they play no role to determine the position of the proton in the baryon spectrum. Only three constituent quarks characterize the baryonic structure of the proton.

This tells that the binding gluons cannot be the constituent of hadrons. As importantly this tells that we can treat the colored valence gluons, just like the quarks, as the constituent particles in QCD. In particular, we can easily construct the color singlet glueballs with two or three valence gluons. This provides a clear picture of the glueballs in QCD and helps us to identify the glueball more clearly [19–21].

A potential problem with this picture of the glueballs is that this could give us too many glueballs, while experimentally we have few candidates of them so far. This is a big mystery in hadron spectroscopy. So the real problem with the glueballs is to understand why there are so few candidates of them experimentally, compared to the rich hadron spectrum based on the successful quark model.

As we have already mentioned, one reason (at least partly) is the possible mixing with the quarkoniums. This makes the experimental identification of glueballs a nontrivial matter. To resolve this problem we need a clear picture of the mixing mechanism, and the Abelian decomposition can easily provide this [24].

Another reason is that the glueballs have an intrinsic instability. To understand this we must understand the confinement mechanism in QCD more clearly, and the Abelian decomposition provides this [25,26]. First, it assures that only the restricted potential can contribute to the Wilson loop integral [27]. This can easily be understood because the valence gluons (being colored) become the confined prisoners, so that only the binding gluons can be the confining agents [20,21]. This, of course, is the Abelian dominance [28].

However, the Abelian dominance does not tell what is the confinement mechanism. This is because the restricted potential is made of two parts, the nontopological Maxwell part and the topological Dirac's monopole part [19,20]. And the Abelian dominance does not tell which part generates the confinement, and how.

Fortunately we can tell which part is responsible for the confinement. Implementing the Abelian decomposition on lattice we can calculate the Wilson loop numerically with the full potential, the restricted potential, and the monopole potential separately, and show that the monopole potential is responsible for the area law in the Wilson loop gauge independently [29–32].

Moreover, we can tell that it is the monopole condensation, more precisely the monopole-antimonopole pair condensation, which generates the confinement in QCD. The Abelian decomposition allows us to calculate the QCD effective action in the presence of the monopole background and establish the stable monopole condensation gauge independently [25,26]. This tells that the true vacuum of QCD is given by the monopole condensation which generates the dimensional transmutation and the mass gap.

This picture of the confinement helps us to understand why there are not so many candidates of the glueballs, because this tells that the glueballs made of the valence gluons have an intrinsic instability. The effective action of QCD tells that the colored gluons, unlike the quarks, tend to annihilate each other in the chromo-electric background. This must be contrasted with quarks, which remain stable inside the hadrons. The reason is that the chromo-electric field tend to create the quark pairs, but annihilate the valence gluons [33–35].

This is closely related to the asymptotic freedom (antiscreening) of gluons. It is well known that in QED the strong electric background tends to generate the pair creation of electrons, which makes the charge screening [36,37]. But in QCD gluons and quarks play opposite roles in the asymptotic freedom. The quarks enhance the screening while the gluons (override the quarks and) diminish it to generate the anti-screening [38,39]. We can understand this with the pair creation of the quarks and the pair annihilation of the valence gluons in the chromo-electric field [25,26].

Clearly the Abelian decomposition predicts new hybrid hadrons made of quarks and valence gluons, in addition to the above glueballs. This is because the valence gluons, just like the quarks, can be viewed as the constituents of (not just the glueballs but) the hadrons. This suggests us to generalize the quark model to the "quark and valence gluon" model, in which both quarks and valence gluons become the constituents of hadrons [19–21].

In this generalization of the quark model we can construct color singlet hadrons from the valence gluons and the valence quarks. For example, we can have a $q\bar{q}g$ color singlet hybrid meson with one octet valence gluon g and a $q\bar{q}$ octet. Or, we can have a $qqqg$ hybrid baryon from the qqq octet and one valence gluon octet g. So the Abelian decomposition of QCD provides a totally new picture of hadron spectroscopy.

Of course, there have been proposals of hybrid hadrons before [40–43]. But a clear picture of hybrid hadrons was missing. The quark and valence gluon model provides a clear picture, and helps us to identify them experimentally.

Finally, the above picture of confinement predicts a totally different type of glueball, the "magnetic" glueball which we can call the "monoball" [20,21]. This is because the monopole condensation could most likely have the vacuum fluctuation which can naturally be identified as a 0^{++} state, which represents the mass gap generated by the monopole condensation. This is the monoball. Clearly this has nothing to do with the above glueballs made of the valence gluons.

The importance of the monoball comes from the fact that it is a direct consequence of the monopole condensation. So the identification of the monoball could be interpreted as the experimental confirmation of the monopole condensation in QCD. This makes the experimental verification of the monoball a most urgent issue in QCD.

Although the quark model has been very successful, PDG tells that there are experimentally established hadronic states which cannot easily be explained by the quark model. For example, the scalar meson $f_0(500)$ or $f_0(980)$ does not seem to fit in the simple quark model, although there have been many efforts to explain this within the quark model [44–46]. We hope that our analysis in this paper will help to identify their physical content more clearly.

The paper is organized as follows. In Sec. II we review the Abelian decomposition and the confinement mechanism for later purpose. In Sec. III discuss the glueball spectrum in QCD. In Sec. IV we discuss the glueball-quarkonium mixing. In Sec. V we present the numerical analysis of the low-lying glueball-quarkonium mixing in 0^{++}, 2^{++}, and 0^{-+} channels. In Sec. VI we briefly discuss the hybrid hadrons in QCD. In Sec. VII we discuss the monoball as the experimental evidence of the monopole condensation in QCD. Finally in the last section we discuss the physical implications of our analysis.

II. BINDING GLUONS AND VALENCE GLUONS: A REVIEW

It is well known that QCD can be understood as the extended QCD (ECD), namely RCD made of the binding gluons which has the valence gluons as colored source [19–21]. This follows from the Abelian decomposition of QCD which decomposes the gauge potential to the restricted part and the valence part gauge independently.

To show this we review the Abelian decomposition first. Consider the SU(2) QCD for simplicity, and let $(\hat{n}_1, \hat{n}_2, \hat{n}_3 = \hat{n})$ be an arbitrary right-handed local orthonormal basis. To make the Abelian decomposition we choose $\hat{n}$ to be the Abelian direction, and impose the isometry to project out the restricted potential $\hat{A}_\mu$ which describes the Abelian sub-dynamics of QCD [19–21]

$$\begin{aligned} &D_\mu \hat{n} = (\partial_\mu + g\vec{A}_\mu \times)\hat{n} = 0, \\ &\vec{A}_\mu \to \hat{A}_\mu = A_\mu \hat{n} - \frac{1}{g}\hat{n}\times\partial_\mu\hat{n} = \mathcal{A}_\mu + \mathcal{C}_\mu, \\ &\mathcal{A}_\mu = A_\mu\hat{n}, \qquad \mathcal{C}_\mu = -\frac{1}{g}\hat{n}\times\partial_\mu\hat{n}, \qquad A_\mu = \hat{n}\cdot\vec{A}_\mu. \end{aligned} \tag{1}$$

This is the Abelian projection which projects out the color neutral binding gluons. Notice that $\hat{A}_\mu$ is precisely the connection which leaves the Abelian direction invariant under the parallel transport. Remarkably, it is made of two parts, the topological (Diracian) $\mathcal{C}_\mu$ which describes the non-Abelian monopole as well as the nontopological (Maxwellian) $\mathcal{A}_\mu$.

Moreover, we have

$$\begin{aligned} &\hat{F}_{\mu\nu} = (F_{\mu\nu} + H_{\mu\nu})\hat{n} = G_{\mu\nu}\hat{n}, \\ &F_{\mu\nu} = \partial_\mu A_\nu - \partial_\nu A_\mu, \\ &H_{\mu\nu} = \partial_\mu C_\nu - \partial_\nu C_\mu, \qquad C_\mu = -\frac{1}{g}\hat{n}_1\cdot\partial_\mu\hat{n}_2, \\ &G_{\mu\nu} = \partial_\mu B_\nu - \partial_\nu B_\mu, \qquad B_\mu = A_\mu + C_\mu. \end{aligned} \tag{2}$$

This tells two things. First, $\hat{F}_{\mu\nu}$ has only the Abelian component. Second, $\hat{F}_{\mu\nu}$ is made of two potentials, the electric (nontopological) A_μ and magnetic (topological) C_μ.

Under the infinitesimal gauge transformation

$$\delta\vec{A}_\mu = \frac{1}{g}D_\mu\vec{\alpha}, \qquad \delta\hat{n}_i = -\vec{\alpha}\times\hat{n}_i, \tag{3}$$

we have

$$\delta A_\mu = \frac{1}{g}\hat{n}\cdot\partial_\mu\vec{\alpha}, \qquad \delta C_\mu = -\frac{1}{g}\hat{n}\cdot\partial_\mu\vec{\alpha}, \tag{4}$$

so that

$$\delta\hat{A}_\mu = \frac{1}{g}\hat{D}_\mu\vec{\alpha}, \qquad (\hat{D}_\mu = \partial_\mu + g\hat{A}_\mu\times). \tag{5}$$

This tells that $\hat{A}_\mu$ has the full SU(2) gauge degrees of freedom, even though it is restricted.

From this we can construct RCD which has the full non-Abelian gauge symmetry but is simpler than the QCD

$$\mathcal{L}_{\mathrm{RCD}} = -\frac{1}{4}\hat{F}_{\mu\nu}^2 = -\frac{1}{4}F_{\mu\nu}^2 + \frac{1}{2g}F_{\mu\nu}\hat{n}\cdot(\partial_\mu\hat{n}\times\partial_\nu\hat{n}) - \frac{1}{4g^2}(\partial_\mu\hat{n}\times\partial_\nu\hat{n})^2, \quad (6)$$

which describes the Abelian subdynamics of QCD. Since RCD contains the non-Abelian monopole degrees explicitly, it provides an ideal platform for us to study the monopole dynamics gauge independently.

With (1) we can recover the full QCD potential adding the non-Abelian (colored) part $\vec{X}_\mu$ [19–21]

$$\vec{A}_\mu = \hat{A}_\mu + \vec{X}_\mu, \qquad \vec{X}_\mu = \frac{1}{g}\hat{n}\times D_\mu\hat{n}, \qquad \hat{n}\cdot\vec{X}_\mu = 0. \quad (7)$$

Under the gauge transformation we have

$$\delta\hat{A}_\mu = \frac{1}{g}\hat{D}_\mu\vec{\alpha}, \qquad \delta\vec{X}_\mu = -\vec{\alpha}\times\vec{X}_\mu. \quad (8)$$

This confirms that $\vec{X}_\mu$ becomes gauge covariant. This is the Abelian decomposition which decomposes the gluons to the color neutral binding gluons and the colored valence gluons gauge independently. This is known as Cho decomposition, Cho-Duan-Ge (CDG) decomposition, or Cho-Faddeev-Niemi (CFN) decomposition [47–50].

From (7) we have

$$\vec{F}_{\mu\nu} = \hat{F}_{\mu\nu} + \hat{D}_\mu\vec{X}_\nu - \hat{D}_\nu\vec{X}_\mu + g\vec{X}_\mu\times\vec{X}_\nu. \quad (9)$$

With this we can express QCD by

$$\mathcal{L}_{\mathrm{QCD}} = -\frac{1}{4}\vec{F}_{\mu\nu}^2 = -\frac{1}{4}\hat{F}_{\mu\nu}^2 - \frac{1}{4}(\hat{D}_\mu\vec{X}_\nu - \hat{D}_\nu\vec{X}_\mu)^2 - \frac{g}{2}\hat{F}_{\mu\nu}\cdot(\vec{X}_\mu\times\vec{X}_\nu) - \frac{g^2}{4}(\vec{X}_\mu\times\vec{X}_\nu)^2. \quad (10)$$

This is the extended QCD (ECD) which confirms that QCD can be viewed as RCD made of the binding gluons, which has the colored valence gluons as its source [19–22].

We can express the Abelian decomposition of the gluons given by (1) and (7) graphically. This is shown in Fig. 1, where the gluons are decomposed to the binding gluons and the valence gluons in (A), and the binding gluons are decomposed further to the nontopological Maxwell part $\mathcal{A}_\mu$ and the topological Dirac part $\mathcal{C}_\mu$ in (B).

The Abelian decomposition of SU(3) QCD is a bit more complicated, but is well known. Since SU(3) has rank two, we have two Abelian subgroups in SU(3). Let $\hat{n}_i (i = 1, 2, \ldots, 8)$ be the local orthonormal SU(3) basis. Clearly we can choose the Abelian directions to be $\hat{n}_3 = \hat{n}$ and $\hat{n}_8 = \hat{n}'$. Now make the Abelian projection by

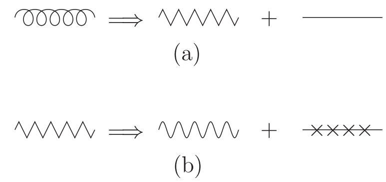

FIG. 1. The Abelian decomposition of the gluons. The gluon is decomposed to the binding gluon (kinked line) and the valence gluon (straight line) in (a), and the binding gluon is further decomposed to the Maxwell part (wiggly line) and Dirac part (spiked line) in (b).

$$D_\mu\hat{n} = 0. \quad (11)$$

This automatically guarantees [51]

$$D_\mu\hat{n}' = 0, \qquad \hat{n}' = \frac{1}{\sqrt{3}}\hat{n}*\hat{n}, \quad (12)$$

where $*$ denotes the d-product. This is because SU(3) has two vector products, the antisymmetric f-product and the symmetric d-product.

Solving (11), we have the following Abelian projection which projects out two neutral binding gluons,

$$\begin{aligned}
\vec{A}_\mu \to \hat{A}_\mu &= A_\mu\hat{n} + A'_\mu\hat{n}' - \frac{1}{g}\hat{n}\times\partial_\mu\hat{n} - \frac{1}{g}\hat{n}'\times\partial_\mu\hat{n}' \\
&= \sum_p \frac{2}{3}\hat{A}_\mu^p, \qquad (p = 1, 2, 3), \\
\hat{A}_\mu^p &= A_\mu^p\hat{n}^p - \frac{1}{g}\hat{n}^p\times\partial_\mu\hat{n}^p = \mathcal{A}_\mu^p + \mathcal{C}_\mu^p, \\
A_\mu^1 &= A_\mu, \qquad A_\mu^2 = -\frac{1}{2}A_\mu + \frac{\sqrt{3}}{2}A'_\mu, \\
A_\mu^3 &= -\frac{1}{2}A_\mu - \frac{\sqrt{3}}{2}A'_\mu, \qquad \hat{n}^1 = \hat{n}, \\
\hat{n}^2 &= -\frac{1}{2}\hat{n} + \frac{\sqrt{3}}{2}\hat{n}', \qquad \hat{n}^3 = -\frac{1}{2}\hat{n} - \frac{\sqrt{3}}{2}\hat{n}',
\end{aligned} \quad (13)$$

where the sum is the sum of the Abelian directions of three SU(2) subgroups made of $(\hat{n}_1, \hat{n}_2, \hat{n}^1), (\hat{n}_6, \hat{n}_7, \hat{n}^2), (\hat{n}_4, -\hat{n}_5, \hat{n}^3)$. Notice the factor 2/3 in front of $\hat{A}_\mu^p$ in the p-summation. This is because the three SU(2) binding potentials are not independent.

From this we have the restricted field strength

$$\hat{F}_{\mu\nu} = \sum_p \frac{2}{3} \hat{F}^p_{\mu\nu}, \tag{14}$$

which is made of two Abelian binding potentials. With this we have the restricted QCD

$$\mathcal{L}_{\mathrm{RCD}} = -\sum_p \frac{1}{6} (\hat{F}^p_{\mu\nu})^2, \tag{15}$$

which has the full SU(3) gauge symmetry. This is because the restricted potential, just as in SU(2), has the full gauge degrees of freedom.

With (13) we have the Abelian decomposition of the SU(3) gauge potential,

$$\begin{aligned}
&\vec{A}_\mu = \hat{A}_\mu + \vec{X}_\mu = \sum_p \left(\frac{2}{3} \hat{A}^p_\mu + \vec{W}^p_\mu \right), \\
&\vec{X}_\mu = \sum_p \vec{W}^p_\mu, \\
&\vec{W}^1_\mu = X^1_\mu \hat{n}_1 + X^2_\mu \hat{n}_2, \qquad \vec{W}^2_\mu = X^6_\mu \hat{n}_6 + X^7_\mu \hat{n}_7, \\
&\vec{W}^3_\mu = X^4_\mu \hat{n}_4 - X^5_\mu \hat{n}_5.
\end{aligned} \tag{16}$$

Here again $\vec{X}_\mu$ transforms covariantly, and can be decomposed to the three valence gluons $\vec{W}^p_\mu$ of the SU(2) subgroups. But unlike $\hat{A}^p_\mu$, they are mutually independent. So we have two binding gluons and six (or three complex) valence gluons in SU(3) QCD.

From (16) we have

$$\begin{aligned}
&\hat{D}_\mu \vec{X}_\nu = \sum_p \hat{D}^p_\mu \vec{W}^p_\nu, \qquad \hat{D}^p_\mu = \partial_\mu + g\hat{A}^p_\mu \times, \\
&\vec{X}_\mu \times \vec{X}_\nu = \sum_{p,q} \vec{W}^p_\mu \times \vec{W}^q_\nu, \\
&\vec{F}_{\mu\nu} = \hat{F}_{\mu\nu} + \hat{D}_\mu \vec{X}_\nu - \hat{D}_\nu \vec{X}_\mu + g\vec{X}_\mu \times \vec{X}_\nu \\
&\quad = \sum_p \left[\frac{2}{3} \hat{F}^p_{\mu\nu} + (\hat{D}^p_\mu \vec{W}^p_\nu - \hat{D}^p_\mu \vec{W}^p_\nu) \right] \\
&\qquad + \sum_{p,q} \vec{W}^p_\mu \times \vec{W}^q_\nu,
\end{aligned} \tag{17}$$

so that we have the following form of SU(3) ECD [25,26]

$$\begin{aligned}
\mathcal{L} &= -\frac{1}{4} \hat{F}^2_{\mu\nu} - \frac{1}{4} (\hat{D}_\mu \vec{X}_\nu - \hat{D}_\nu \vec{X}_\mu)^2 - \frac{g}{2} (\hat{D}_\mu \vec{X}_\nu - \hat{D}_\nu \vec{X}_\mu) \cdot (\vec{X}_\mu \times \vec{X}_\nu) - \frac{g}{2} \hat{F}_{\mu\nu} \cdot (\vec{X}_\mu \times \vec{X}_\nu) - \frac{g^2}{4} (\vec{X}_\mu \times \vec{X}_\nu)^2 \\
&= \sum_p \left\{ -\frac{1}{6} (\hat{F}^p_{\mu\nu})^2 - \frac{1}{4} (\hat{D}^p_\mu \vec{W}^p_\nu - \hat{D}^p_\nu \vec{W}^p_\mu)^2 - \frac{g}{2} \hat{F}^p_{\mu\nu} \cdot (\vec{W}^p_\mu \times \vec{W}^p_\nu) \right\} - \sum_{p,q} \frac{g^2}{4} (\vec{W}^p_\mu \times \vec{W}^q_\mu)^2 \\
&\quad - \sum_{p,q,r} \frac{g}{2} (\hat{D}^p_\mu \vec{W}^p_\nu - \hat{D}^p_\nu \vec{W}^p_\mu) \cdot (\vec{W}^q_\mu \times \vec{W}^r_\mu) - \sum_{p \neq q} \frac{g^2}{4} ((\vec{W}^p_\mu \times \vec{W}^q_\nu) \cdot (\vec{W}^q_\mu \times \vec{W}^p_\nu) + (\vec{W}^p_\mu \times \vec{W}^p_\nu) \cdot (\vec{W}^q_\mu \times \vec{W}^q_\nu)).
\end{aligned} \tag{18}$$

This shows that the interactions in SU(3) QCD are more complicated than the SU(2) QCD. But what is remarkable about (18) is that it is Weyl symmetric, symmetric under the permutation of the three SU(2) subgroups of SU(3).

We can easily add quarks in the Abelian decomposition,

$$\begin{aligned}
\mathcal{L}_q &= \sum_k \bar{\Psi}_k (i\gamma^\mu D_\mu - m) \Psi_k \\
&= \sum_k \left[\bar{\Psi}_k (i\gamma^\mu \hat{D}_\mu - m) \Psi_k + \frac{g}{2} \vec{X}_\mu \cdot \bar{\Psi}_k (\gamma^\mu \vec{t}) \Psi_k \right] \\
&= \sum_{p,k} \left[\bar{\Psi}^p_k (i\gamma^\mu \hat{D}^p_\mu - m) \Psi^p_k + \frac{g}{2} \vec{W}^p_\mu \cdot \bar{\Psi}^p_k (\gamma^\mu \vec{\tau}^p) \Psi^p_k \right], \\
\hat{D}_\mu &= \partial_\mu + \frac{g}{2i} \vec{t} \cdot \hat{A}_\mu, \qquad \hat{D}^p_\mu = \partial_\mu + \frac{g}{2i} \vec{\tau}^p \cdot \hat{A}^p_\mu,
\end{aligned} \tag{19}$$

where m is the mass, k and p denote the flavor and color of the quarks, and Ψ^p_k represents the three SU(2) quark doublets [i.e., (r, b), (b, g), and (g, r) doublets] of the (r, b, g) quark triplet.

From this it becomes obvious that the binding gluons and the valence gluons play different roles. So from now on we will call the binding gluon the "neuron" (or "neuton") and the valence gluon the "chromon" (or "coloron").

To assign the color to the chromons, let (r, g, b) be the colors of three quarks. Then the colors of the six chromons are given by $(r\bar{b}, b\bar{g}, g\bar{r}, \bar{r}b, \bar{b}g, \bar{g}r)$, which we denote for simplicity by $(R, B, G, \bar{R}, \bar{B}, \bar{G})$. This is schematically shown in Fig. 2.

We can show how the Abelian decomposition refines QCD interaction graphically. This is shown in Fig. 3. In (A) the three-point QCD gluon vertex is decomposed to two vertices made of one neuron and two chromons and three chromons. In (B) the four-point gluon vertex is decomposed to three vertices made of one neuron and three chromons, two neurons and two chromons, and four

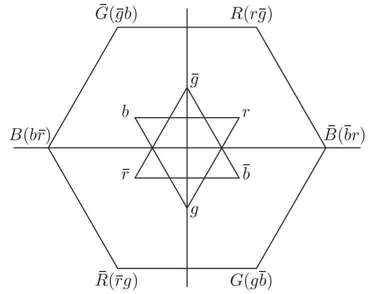

FIG. 2. The color assignment of quarks and chromons. The x-axis and y-axis represent the λ_3 and λ_8 quantum numbers.

chromons. In (C) the quark-gluon vertex is decomposed to the quark-neuron vertex and quark-chromon vertex.

Notice that here (and in the following figures) the neurons are expressed by the wiggly lines (Maxwell part). This is because the monopole potential (Dirac part) makes the condensation, so that in the perturbative regime (inside the hadrons) it does not contribute to the Feynman diagrams. Also here three-point vertex made of three neurons or two neurons and one chromon, and four-point vertex made of three or four neurons are forbidden by the conservation of color. Moreover, the quark-neuron interaction does not change the quark color, but the quark-chromon interaction changes the quark color.

An important implication of Fig. 3 is that there are two types of gluon jets, the neuron jet and chromon jet. In principle we can test this experimentally by studying the gluon jets. Experiments can tell the difference between the photon-quark jet from the gluon-quark jet. If so, by (re-) analyzing the gluon-gluon jets and/or gluon-quark jets more carefully we could confirm that indeed there are two types of gluon jets. Experimental confirmation of this

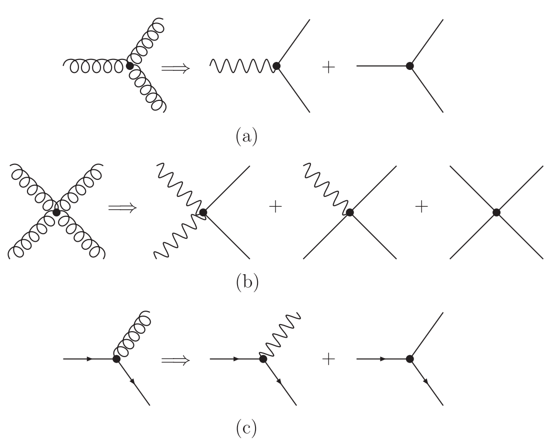

FIG. 3. The decomposition of vertices in SU(3) QCD. The three and four point gluon vertices are decomposed in (a) and (b), and the quark gluon vertices are decomposed in (c). Notice that here (and in the following) the neurons are represented by wiggly lines and the chromons are represented by straight lines.

is very important, because this could endorse the existence of two types of gluons.

Our analysis tells that, although the Abelian decomposition does not change QCD, it makes many hidden structures of QCD explicit. First, it tells that RCD is responsible for the confinement, because the valence gluons (being colored) have to be confined [27,28]. So it makes the Abelian dominance obvious.

Second, it allows us to prove that the monopole is responsible for the area law in the Wilson loop integral. Indeed implementing (11) on lattice, two lattice QCD groups (the SNU-KU and KEK-CU groups) independently performed a truly gauge independent lattice calculation, and showed that the monopole is responsible for the confinement [29–32]. The SNU-KU result is shown in Fig. 4, which shows that the full gauge potential, the restricted potential, and the monopole potential all produce the linear confining potential in Wilson loop integral. This assures that we only need the monopole potential for the confining force.

Moreover, the Abelian decomposition enlarges and doubles the gauge symmetry to the classical and the quantum gauge symmetries, because it automatically puts QCD in the background field formalism [52,53]. So the neurons and the chromons have independent gauge freedoms. This keeps both neurons and chromons massless.

Third, it reduces the complicated non-Abelian gauge symmetry to a simple discrete symmetry called the color reflection invariance. To see this, consider the rotation of basis called the color reflection in SU(2) QCD

$$(\hat{n}_1, \hat{n}_2, \hat{n}) \rightarrow (\hat{n}_1, -\hat{n}_2, -\hat{n}). \tag{20}$$

Obviously this is a gauge transformation, so that this must remain a symmetry of QCD. On the other hand, the isometry condition (1) does not change under (20). This means that, after we select the Abelian direction $\hat{n}$ we have two different but gauge equivalent Abelian decompositions related by the color reflection.

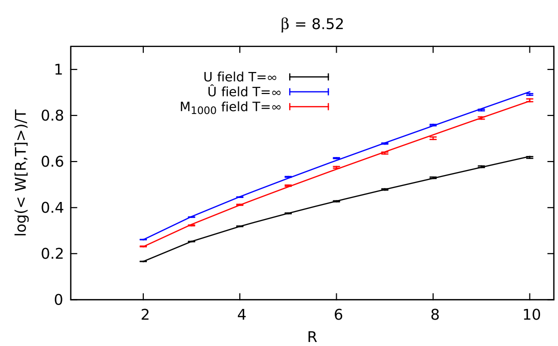

FIG. 4 (color online). The lattice QCD calculation which establishes the monopole dominance in Wilson loop. Here the black, red, and blue slopes are obtained with the full potential, the restricted potential, and the monopole potential, respectively.

What makes the color reflection symmetry so important is that it is the only remaining symmetry of the full gauge symmetry left over, after we make the Abelian decomposition [20,21]. So the color reflection invariance plays the role of the non-Abelian gauge invariance after we have chosen the Abelian direction. This greatly simplifies the implementation of the gauge invariance to calculate the QCD effective action [25,26].

In the constant monopole background the effective action is given by

$$\mathcal{L}_{\rm eff} = -\sum_p \left(\frac{H_p^2}{3} + \frac{11g^2}{48\pi^2} H_p^2 \left(\ln \frac{gH_p}{\mu^2} - c \right) \right). \tag{21}$$

where $H_p (p = 1, 2, 3)$ are the monopole background of three SU(2) subgroups. The corresponding effective potential has the true minimum at

$$\langle H_1 \rangle = \langle H_2 \rangle = \langle H_3 \rangle = \frac{\mu^2}{g} \exp\left(-\frac{16\pi^2}{11g^2} + \frac{3}{4} \right). \tag{22}$$

The effective potential is shown in Fig. 5. This demonstrates the monopole condensation which generates the desired mass gap in QCD.

For the constant chromo-electric background we have the following effective action

$$\mathcal{L}_{\rm eff} = \sum_p \left(\frac{E_p^2}{3} + \frac{11g^2}{48\pi^2} E_p^2 \left(\ln \frac{gE_p}{\mu^2} - c \right) - i \frac{11g^2}{96\pi} E_p^2 \right).$$

Notice that it has the imaginary part which is negative. This is very important, because this tells that the chromo-electric background induces the pair annihilation of chromons [25,26,33–35].

To summarize, the Abelian decomposition tells that QCD has two gluons which play different roles. Perturbatively (in terms of the Feynman diagrams) the neurons play the role of the photon and the chromons play the role of (massless) charged vector fields, in QED. Nonperturbatively, however, (the monopole part of) the neurons become the confining agents. In contrast, the chromons become the confined prisoners. Without the Abelian decomposition we cannot tell this difference because all gluons are treated on equal footing.

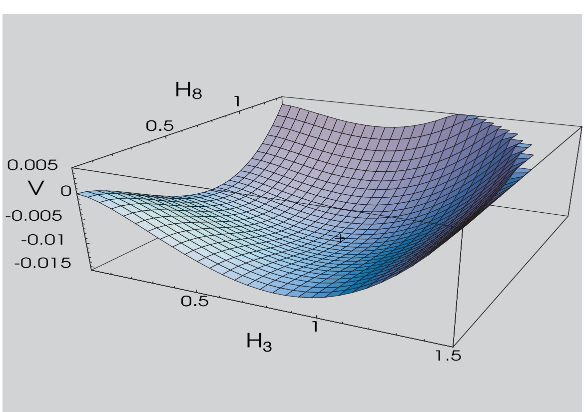

FIG. 5 (color online). The effective potential of SU(3) QCD.

III. GLUEBALLS AND ODDBALLS

The fact that the chromons become gauge covariant tells that they could form glueballs. For example, we can have the $g\bar{g}$ or ggg color singlet glueballs made of chromons which could be called the "chromoballs."

Since we have six gauge covariant chromons $(R_\mu, B_\mu, G_\mu, \bar{R}_\mu, \bar{B}_\mu, \bar{G}_\mu)$, we can construct low-lying color singlet glueballs with two $(g\bar{g})$ chromons whose wave functions are symmetric under the exchange

$$|g\bar{g}\rangle = \frac{|R_\mu \bar{R}_\nu\rangle + |B_\mu \bar{B}_\nu\rangle + |G_\mu \bar{G}_\nu\rangle}{\sqrt{3}}. \tag{23}$$

The low-lying $g\bar{g}$ glueball states classified by ${}^{(2S+1)}L_J$ are shown in Table I. In the table we have listed the possible candidates of the glueballs based on the PDG data, but we emphasize that they are by no means certain.

Actually the number of the glueball states depends on how many degrees the chromons have. If we assume the chromons to be massless they have only transversal degrees, but if we assume them massive they also have the longitudinal degrees. Here we have assumed that they acquire the (constituent) mass after the confinement sets in. But ultimately experiments should determine how many degrees the chromons have.

Similarly we can construct low-lying color singlet glueballs with three chromons,

$$|ggg\rangle_d = \frac{\sum_{(RGB)} |R_\mu B_\nu G_\rho\rangle}{\sqrt{6}},$$
$$|ggg\rangle_f = \frac{\sum_{[RGB]} |R_\mu B_\nu G_\rho\rangle}{\sqrt{6}}, \tag{24}$$

TABLE I. The possible quantum numbers for low-lying glueballs made of two chromons.

${}^{(2S+1)}L_J$	J^{PC}	possible candidates
${}^1S_0$	0^{++}	$f_0(500), f_0(980)$
${}^5S_2$	2^{++}	$f_2(1950)$
${}^3P_0$	0^{-+}	$\eta(1295), \eta(1405), \eta(1475)$
${}^3P_1$	1^{-+}	???
${}^3P_2$	2^{-+}	$\eta_2(1645)$
${}^1D_2$	2^{++}	Regge recurrence of ${}^1S_0$
${}^5D_0$	0^{++}	$f_0(1500)$
${}^5D_1$	1^{-+}	???
${}^5D_2$	2^{++}	Regge recurrence of ${}^5S_2$

TABLE II. The possible quantum numbers for low-lying glueballs made of three chromons. Here S, A, and M mean symmetric, antisymmetric, and mixed symmetries, and d and f mean (totally symmetric) d-product and (totally antisymmetric) f-product of three chromons.

Configuration	space	spin	color	L	S	J^{PC}
$(1s)^3$	S	S	d	0	1, 3	$1^{--}, 3^{--}$
	S	A	f	0	0	0^{-+}
$(1s)^2(1p)$	S	S	d	1	1, 3	$(0,1,2)^{+-}, (2,3,4)^{+-}$
	S	A	f	1	0	1^{++}
	M	M	d	1	1, 2	$(0,1,2)^{+-}, (1,2,3)^{+-}$
	M	M	f	1	1, 2	$(0,1,2)^{++}, (1,2,3)^{++}$
$(1s)(1p)^2$	S	S	d	0,2	1, 3	$(1,2,3,4,5)^{--}$
	S	A	f	0,2	0	$0^{-+}, 2^{-+}$
	M	M	d	0,2	1, 2	$(0,1,2,3,4)^{--}$
	M	M	f	0,2	1, 2	$(0,1,2,3,4)^{-+}$
	M	M	d	1	1, 2	$(0,1,2,3)^{--}$
	M	M	f	1	1, 2	$(0,1,2,3)^{-+}$
	A	S	d	1	1, 3	$(0,1,2,3,4)^{-+}$
	A	A	f	1	0	1^{--}
$(1s)^2(2s)$	S	S	d	0	1, 3	$1^{--}, 3^{--}$
	S	A	f	0	0	0^{-+}
	M	M	d	0	1, 2	$(1,2)^{--}$
	M	M	f	0	1, 2	$(1,2)^{-+}$
$(1s)^2(1d)$	S	S	d	2	1, 3	$(1,2,3,4,5)^{--}$
	S	A	f	2	0	2^{-+}
	M	M	f	2	1, 2	$(0,1,2,3,4)^{--}$
	M	M	f	2	1, 2	$(0,1,2,3,4)^{-+}$

where the sums in ggg are the totally symmetric (the d-product) and the totally antisymmetric (the f-product) combination of three colors.

With this one can figure out the possible ggg chromoball states. The exact enumeration of three chromon bound states depends on the binding potential, but in a simple shell model one can construct the low-lying ggg chromoball states [6]. This is shown in Table II. In general the ggg glueballs are expected to be heavier than the gg glueballs, because they have more chromons.

At this point one might wonder if the neurons could also form bound states. Certainly from the group theoretic point of view we could construct color singlet states with two or three neurons. This, however, does not guarantee that dynamically the neurons can make bound states. Since they carry no color charge the interaction among them should be very weak, so that they are not likely to form bound states.

To clarify this point, consider the photons in QED. Clearly they interact among themselves through the electron loops, but obviously they do not form bound states. Here the situation is very similar, because the neurons in QCD are exactly like the photons in QED. To amplify this point we show the possible interactions among neurons in Fig. 6. This is precisely the photon interaction of QED made of the charged vector field.

From this we may conclude that the neurons do not make bound states. Indeed the Feynman diagram tells that, if such a bound state exists at all in QCD, it could be interpreted as a bound state of two quarkoniums.

This should be compared with the possible Feynman diagram of the chromoball interactions shown in Fig. 7. The contrast between the two Feynman diagrams are unmistakable. We emphasize that, without the Abelian decomposition, it would have been very difficult to see this difference.

The above analysis tells that there must be a large number of glueballs. But experimentally we do not have many candidates of them. As we have remarked, one reason is that these glueballs may not exist as mass eigenstates,

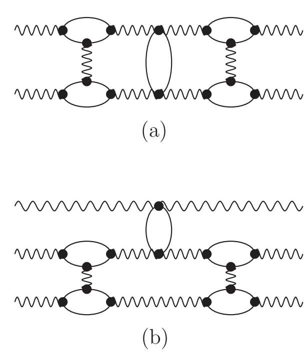

FIG. 6. The possible Feynman diagrams of the neuron interaction. Two neuron binding is shown in (a), and three neuron binding is shown in (b).

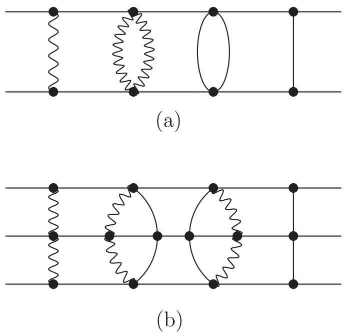

FIG. 7. The possible Feynman diagrams which bind the chromons. Two chromon binding is shown in (a), three chromon binding is shown in (b).

because they could mix with $q\bar{q}$ states. So it is very important to discuss the glueball-quarkonium mixing to identify these glueballs.

Another reason is that the chromoballs (unlike the quarkoniums) have an intrinsic instability, because they tend to annihilate each other in strong chromo-electric field [25,26]. This is due to the anti-screening and asymptotic freedom [38,39].

We can estimate the glueball partial decay width coming from this instability. According to the QCD one-loop effective action (23) the chromon annihilation probability per unit volume per unit time is given by

$$\Gamma_A = \sum_p \frac{11g^2}{96\pi} \bar{E}_p^2 \times \frac{4\pi}{3\Lambda_{\rm QCD}^3}, \tag{25}$$

where the sum is on three SU(2) subgroups and $\bar{E}_p$ is the average chromo-electric field of each subgroup inside the glueballs. Now, if we choose $\alpha_s \simeq 0.4$, $\Lambda_{\rm QCD} \simeq 339$ MeV (for three quark flavors), and $\bar{E}_p \simeq (g/\pi)\Lambda_{\rm QCD}^2$ we have $\Gamma_A \simeq 398$ MeV [17]. But notice that with $\Lambda_{\rm QCD} \simeq$ 200 MeV, we have $\Gamma_A \simeq 235$ MeV [54].

Of course this is a rough estimate, but notice that this is the partial decay width we expect from the asymptotic freedom, in addition to the "normal" hadronic decay width. This strongly implies that in general the glueballs (in particular excited ones) are expected to be quite unstable. As we have remarked this could be one of the reasons why there are so few candidates of glueballs experimentally.

Although the glueballs in general mix with the quarkoniums, in particular cases the pure glueballs could exist [6]. This is because some of the $g\bar{g}$ glueballs have the quantum number J^{PC} which $q\bar{q}$ cannot have. In the quark model the $q\bar{q}$ states in the natural spin-parity series $P = (-1)^J$ must have spin one, and hence $CP = +1$. So the mesons with natural spin-parity and $CP = -1$ (e.g., $0^{--}, 0^{+-}, 1^{-+}, 2^{+-}$, etc.) are forbidden. But the $g\bar{g}$ or ggg glueballs could have these quantum states. In fact, the ggg glueballs, unlike $q\bar{q}$, could have all possible J^{PC}.

So these particular glueballs carrying the quantum numbers which $q\bar{q}$ cannot have cannot mix with the quarkoniums, and they are called the "oddballs" [6]. The low-lying oddballs become important because they could be observed as pure glueball states. Table III summarizes the possible J^{PC} for the $q\bar{q}$, $g\bar{g}$, and ggg states. From this we can say definitely that any of the low-lying $0^{+-}, 0^{--}, 1^{-+}$, or 2^{+-} meson states must be pure glueballs. This could provide crucial information for us to search for the pure glueballs.

The above analysis tells that the identification of the glueballs may not be simple. To identify these glueball states we have to compare the theoretical prediction with the experimental data. In the Appendix we show two tables, the one which provides the standard quark model interpretation of the low-lying mesons and the other which contains the light isosinglet mesons which cannot easily be identified as $q\bar{q}$ states, from PDG data [17].

IV. GLUEBALL-QUARKONIUM MIXING

To identify the glueballs we have to study their mixing with the quarkoniums. But before we discuss the mixing, it is worth discussing the $q\bar{q}$ octet-singlet mixing in the quark model first.

The $q\bar{q}$ binding energy may come from two orthogonal processes, the exchange and annihilation processes. Let us assume [24]

$$\begin{aligned} \langle u\bar{u}|H|u\bar{u}\rangle_{Ex} &= \langle d\bar{d}|H|d\bar{d}\rangle_{Ex} = E, \\ \langle s\bar{s}|H|s\bar{s}\rangle_{Ex} &= E' = E + \Delta, \\ \langle q'\bar{q}'|H|q\bar{q}\rangle_{An} &= A, \qquad (\text{for all } q, q'). \end{aligned} \tag{26}$$

Now with

$$\begin{aligned} |8\rangle &= \frac{|u\bar{u}\rangle + |d\bar{d}\rangle - 2|s\bar{s}\rangle}{\sqrt{6}}, \\ |1\rangle &= \frac{|u\bar{u}\rangle + |d\bar{d}\rangle + |s\bar{s}\rangle}{\sqrt{3}}, \end{aligned} \tag{27}$$

TABLE III. The possible quantum numbers for low-lying the $q\bar{q}$, $g\bar{g}$, and ggg states.

State	$q\bar{q}$	$g\bar{g}$	ggg	State	$q\bar{q}$	$g\bar{g}$	ggg
State	$q\bar{q}$	$g\bar{g}$	ggg	State	$q\bar{q}$	$g\bar{g}$	ggg
0^{++}	O	O	O	2^{++}	O	O	O
0^{+-}	X	X	O	2^{+-}	X	X	O
0^{-+}	O	O	O	2^{-+}	O	O	O
0^{--}	X	X	O	2^{--}	O	X	O
1^{++}	O	O	O	3^{++}	O	O	O
1^{+-}	O	X	O	3^{+-}	O	X	O
1^{-+}	X	O	O	3^{-+}	X	O	O
1^{--}	O	X	O	3^{--}	O	X	O

we may obtain the following mass matrix for the $q\bar{q}$ which describes the octet-singlet mixing,

$$M^2 = \begin{pmatrix} \langle 8|H|8\rangle & \langle 8|H|1\rangle \\ \langle 1|H|8\rangle & \langle 1|H|1\rangle \end{pmatrix} = \begin{pmatrix} E + \frac{2}{3}\Delta & -\frac{\sqrt{2}}{3}\Delta \\ -\frac{\sqrt{2}}{3}\Delta & E + \frac{1}{3}\Delta + 3A \end{pmatrix}. \quad (28)$$

Notice that Δ-term is responsible for the mixing.

From this we have the mass eigenvalues

$$m_{\pm}^2 = \frac{1}{2}[(E' + E + 3A) \pm D], \quad D = \sqrt{(E' - E - A)^2 + 8A^2}. \quad (29)$$

Notice that (when A is positive) the eigenvalues $m_{\pm}^2$ must satisfy $m_-^2 < E$ and $E' < m_+^2$. This tells us that the annihilation contribution has a tendency to make the mass splitting larger, which seems to be the case in reality.

Now we can discuss the glueball-quarkonium mixing. The possible Feynman diagrams for the mixing is shown in Fig. 8. From this it is clear that the mixing takes place not just between the quarkoniums and glueballs but also between the gg and ggg glueballs, directly or through the virtual states made of neurons.

To proceed, let $|G\rangle$ be the glueball state which mixes with two quarkonium states $|8\rangle, |1\rangle$ and consider the mass matrix of $(|8\rangle, |1\rangle, |G\rangle)$,

$$\mathcal{M} = \begin{pmatrix} a & b & 0 \\ b & c & d \\ 0 & d & e \end{pmatrix}, \quad (30)$$

whose eigenvalues are given by λ_i. In this case the mixing matrix $\mathcal{U}$ which transforms the unphysical states to the physical states $(|m_1\rangle, |m_2\rangle, |m_3\rangle)$ and diagonalizes $\mathcal{M}$ to $\mathcal{D}$ is given by [24]

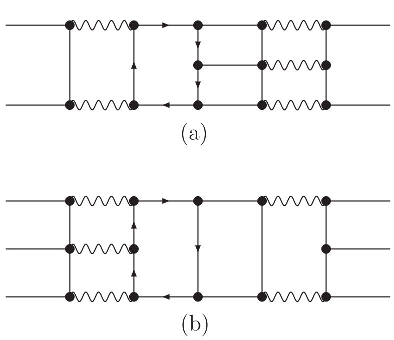

FIG. 8. The possible glueball-quarkonium mixing diagrams. The mixing of glueballs made of two and three chromons with quarkoniums are shown in (a) and (b).

$$\mathcal{D} = \mathcal{U}M\mathcal{U}^\dagger = \mathrm{diag}(\lambda_1, \lambda_2, \lambda_3),$$

$$\mathcal{U} = \begin{pmatrix} \frac{b(\lambda_1 - e)}{d(\lambda_1 - a)}\alpha_1, & \frac{\lambda_1 - e}{d}\alpha_1, & \alpha_1 \\ \frac{b(\lambda_2 - e)}{d(\lambda_2 - a)}\alpha_2, & \frac{\lambda_2 - e}{d}\alpha_2, & \alpha_2 \\ \frac{b(\lambda_3 - e)}{d(\lambda_3 - a)}\alpha_3, & \frac{\lambda_3 - e}{d}\alpha_3 & \alpha_3 \end{pmatrix},$$

$$\alpha_i = \frac{d}{(\lambda_i - e)\sqrt{1 + (\frac{b}{\lambda_i - a})^2 + (\frac{d}{\lambda_i - e})^2}}. \quad (31)$$

Moreover, we have the sum rules

$$a + c + e = \lambda_1 + \lambda_2 + \lambda_3,$$
$$ac + ce + ea - b^2 - d^2 = \lambda_1\lambda_2 + \lambda_2\lambda_3 + \lambda_3\lambda_1,$$
$$ace - b^2 e - d^2 a = \lambda_1\lambda_2\lambda_3. \quad (32)$$

Notice that α_i determines the gluon content of physical states.

The gluon content of the physical states has important implication. For example, this allows us to predict the relative branching ratios of ψ to γX decays among the physical states. This is because the ψ decay process to ordinary noncharming physical states is the Okubo-Zweig-Iizuka (OZI) suppressed process which can only be made possible through the gluons.

So, except for the kinematic phase factor, the glue content of the physical states determines the radiative decay branching ratios. This means that for the S wave decay (i.e., for 0^{++} and 2^{++}) we have

$$R\left(\frac{\psi \to \gamma X_k}{\psi \to \gamma X_i}\right) = \left(\frac{\alpha_k}{\alpha_i}\right)^2 \left(\frac{m_\psi^2 - m_k^2}{m_\psi^2 - m_i^2}\right)^3, \quad (33)$$

but for the P wave decay (i.e., for 0^{-+}) we expect to have

$$R\left(\frac{\psi \to \gamma X_k}{\psi \to \gamma X_i}\right) = \left(\frac{\alpha_k}{\alpha_i}\right)^2 \left(\frac{m_\psi^2 - m_k^2}{m_\psi^2 - m_i^2}\right)^5, \quad (34)$$

where the last term is the kinematic phase space factor. So the gluon content of the physical states can explain the underlying dynamics of the OZI rule.

Of course the idea of the glueball-quarkonium mixing has been suggested many times before [6,55,56]. But the clear picture of the mixing was lacking because the constituent gluons were not well defined. The quark and chromon model allows us to discuss the mixing without any ambiguity [24].

V. EXAMPLES OF MIXING: NUMERICAL ANALYSIS

To discuss the mixing notice that, among the five low-lying $g\bar{g}$ states ($^1S_0, ^5S_2, ^3P_0, ^3P_1, ^3P_2$ states) in Table I there are three glueball states (i.e., $0^{++}, 2^{++}$, and

0^{-+} states) which can easily mix with the low-lying quarkonium states. So in this section we will restrict ourselves to the mixing of these glueball states with the corresponding isosinglet $q\bar{q}$ states below 2 GeV—with the light quarks u, d, and s only—for simplicity.

In this approximation the mass matrix of the mixing can be written as

$$M^2 = \begin{pmatrix} E + \frac{2}{3}\Delta & -\frac{\sqrt{2}}{3}\Delta & 0 \\ -\frac{\sqrt{2}}{3}\Delta & E + \frac{1}{3}\Delta + 3A & \nu \\ 0 & \nu & G \end{pmatrix}. \tag{35}$$

It has five parameters, but we can fix E and Δ from the $q\bar{q}$ octet-singlet mixing. So we need three inputs to fix the mass matrix completely.

There are different ways to fix the mass matrix. One way is to choose two predominantly $q\bar{q}$ states, or simply to choose two lowest mass eigenstates, from PDG. With this we could treat G as a free parameter, and find (if possible) the best fit for G which could explain the PDG data. In this case we can replace G with the chromon constituent mass μ writing $G = 4\mu^2$, since G represents the mass of two chromons.

Another way to fix the mass matrix is to notice that in this approximation we may assume

$$\langle q'\bar{q}'|H|q\bar{q}\rangle_{An} \simeq \langle q'\bar{q}'|gg\rangle\langle gg|q\bar{q}\rangle. \tag{36}$$

So, instead of varying μ we could impose the condition $3A = \nu^2$ to fix the mass matrix. But this requirement could be too stringent, and we will not require this in this paper.

We emphasize the clarity of our mixing mechanism presented by the quark and chromon model. All terms in (35) have clear physical meaning. For example, we can draw the Feynman diagram which represents the isosinglet-glueball mixing parameter ν, and could in principle calculate it theoretically.

With this we can predict the mass of the third state, calculate the quark and gluon contents of the physical states, and the relative branching ratios of the ψ radiative decay to the physical states in each channel (in terms of μ if necessary).

With this strategy we now can discuss the glueball-quarkonium mixing in each channel separately. According to PDG the low-lying iso-singlet physical states in the 0^{++} and 2^{++} channels below 2 GeV are $f_0(500), f_0(980), f_0(1370), f_0(1500), f_0(1710)$ and $f_2(1270), f_2{}'(1525), f_2(1950)$. In the 0^{-+} channel we have $\eta(548), \eta'(958), \eta(1295), \eta(1405), \eta(1475)$ and $\eta(1760)$ [17]. These are the subjects of our analysis in the following.

A. 0^{++} channel

In this channel one would normally assume $a_0(980)$ to be the isotriplet partner of the isosinglet $q\bar{q}$ and choose

$$\begin{aligned} &E = a_0^2, \qquad a_0 = a_0(980), \\ &\Delta = 2(K^2 - a_0^2), \qquad K = K_0^*(1430). \end{aligned} \tag{37}$$

This seems natural because $a_0(980)$ which is supposed to be made of u and d quarks is lighter than $K_0^*(1430)$ made of s quark.

On the other hand PDG interprets $a_0(980)$ [as well as $f_0(500)$ and $f_0(980)$] to be a meson-meson bound state, and suggests the following choice [17]

$$\begin{aligned} &E = a_0^2, \qquad a_0 = a_0(1450), \\ &\Delta = 2(K^2 - a_0^2), \qquad K = K_0^*(1430). \end{aligned} \tag{38}$$

This looks somewhat strange because this implies that the $q\bar{q}$ state made of $u + d$ quark is heavier (or at least not lighter) than the $q\bar{q}$ state made of the s quark.

Clearly the numerical analysis of the mixing will depend very much on which input we use, and it is not clear which view is correct. But here we will simply adopt the PDG suggestion and use (38) as the input in our analysis.

With this we have three undetermined parameters in the mass matrix. To fix them we may choose two physical states from PDG, and vary the chromon mass μ as an independent parameter. But here we have five physical states, $f_0(500), f_0(980), f_0(1370), f_0(1500)$, and $f_0(1710)$ below 2 GeV. Since the identity of $f_0(500)$ and $f_0(980)$ are not clear we will choose $f_0(1500)$ and $f_0(1710)$ as the input. In this case we obtain Table IV. Notice that we have calculated $\zeta = \nu^2/A$ to see how good is the constraint $3A = \nu^2$ in this approximation.

The numerical result suggests that the mass of the third state is around 1400 MeV which is predominantly a $s\bar{s}$ state, which we could interpret to be $f_0(1370)$. Interestingly, the physical contents of two other states depend very much on the value of the chromon mass μ. When the mass is around 760 MeV, $f_0(1500)$ become predominantly the glue state. But as the chromon mass increases to 860 MeV, it becomes a $u + d$ state and $f_0(1710)$ quickly becomes the glue state.

So when the chromon mass is around 760 MeV the above result appears to be in agreement with the suggestion of PDG, which lists $f_0(1370)$ and $f_0(1710)$ as the $q\bar{q}$ states [17]. But here again the $q\bar{q}$ state made of s quark becomes lighter than the $q\bar{q}$ state made of $u + d$. This, of course, is due to the input (38).

In principle we could determine the chromon mass with our prediction of the relative ratio of the ψ radiative decay. Unfortunately at the moment PDG has no experimental data available for us to do this.

TABLE IV. The predicted mass of the third physical state, the quark and glue component (the probability) of the physical states, and the relative radiative decay ratios for fixed values of the gluon mass μ in the 0^{++} channel. Here we choose $f_0(1500)$ and $f_0(1710)$ as the input.

					$m_1 = f_0(1500)$			$m_2 = f_0(1710)$			m_3				
μ	A	ν	ζ	m_3	$u+d$	s	g	$u+d$	s	g	$u+d$	s	g	$R(m_2/m_1)$	$R(m_3/m_1)$
0.76	0.27	0.18	0.12	1.40	0.07	0.00	0.93	0.73	0.20	0.07	0.19	0.80	0.00	0.00	0.05
0.78	0.23	0.31	0.42	1.40	0.26	0.01	0.73	0.59	0.16	0.25	0.15	0.83	0.02	0.02	0.14
0.80	0.18	0.36	0.69	1.39	0.44	0.01	0.54	0.45	0.12	0.43	0.11	0.87	0.02	0.05	0.59
0.82	0.14	0.35	0.90	1.39	0.62	0.02	0.36	0.30	0.08	0.62	0.09	0.90	0.01	0.07	1.26
0.84	0.09	0.29	0.92	1.39	0.79	0.02	0.18	0.15	0.04	0.80	0.05	0.93	0.01	0.09	3.26
0.86	0.04	0.07	0.12	1.39	0.96	0.03	0.01	0.01	0.00	0.99	0.03	0.97	0.00	0.12	85.71

B. 2^{++}channel

In this channel we have three physical states below 2 GeV, $f_2(1270)$, $f_2{}'(1525)$, and $f_2(1950)$. Of course, we also have $f_2(1430)$, $f_2(1565)$, $f_2(1640)$, $f_2(1810)$, and $f_2(1910)$, but we will not consider them here because PDG does not classify them as established states. On the other hand the fact that there are so many candidates of 2^{++} states implies that we need more caution to analyze this channel.

Now, we can choose

$$E = a_2^2, \qquad a_2 = a_2(1320),$$
$$\Delta = 2(K^{*2} - a_2^2), \qquad K^* = K^*(1430), \tag{39}$$

as the input and vary the chromon mass μ as a free parameter. In this case we have three possibilities to choose two input states from $f_2(1270)$, $f_2{}'(1525)$, and $f_2(1950)$.

With $f_2(1270)$ and $f_2(1950)$ as the input, we obtain Table V. Notice that when $\mu \simeq 760$ MeV, we have $m_3 \simeq 1,470$ MeV which could be identified as $f'(1525)$. In this case $f_2(1270)$ becomes a mixture of $u+d$ and glue states, and $f_2(1950)$ becomes a mixture of $u+d$, s and glue states. But the third physical state $f'(1525)$ becomes predominantly an $s\bar{s}$ state.

But when the chromon mass μ becomes around 860 MeV, $f_2(1270)$ becomes predominantly $u+d$ state and the third state $f_2{}'(1525)$ becomes predominantly $s\bar{s}$ state. This is in line with the PDG suggestion, which interprets $f_2(1270)$ and $f_2{}'(1525)$ as the $q\bar{q}$ states [17].

Experimentally, PDG shows

$$J/\Psi \to \gamma f_2(1270) \simeq (1.43 \pm 0.11) \times 10^{-3}$$
$$J/\Psi \to \gamma f_2{}'(1525) \simeq (4.5 + 0.7 - 0.4) \times 10^{-4},$$

which implies

$$R(f_2{}'(1525)/f_2(1270)) \simeq 0.31 \pm 0.05. \tag{40}$$

Remarkably this agrees excellently with our prediction in Table V, when the chromon mass becomes 860 MeV. So all in all the mixing in this channel seems to work very well, although we certainly need a more careful analysis.

C. 0^{-+} channel

In this channel we have six physical states below 2 GeV, $\eta(548), \eta'(958), \eta(1295), \eta(1405), \eta(1475)$, and $\eta(1760)$. But here we need a special attention because of the expected difficulties [the $U(1)$ problem, PCAC, etc.] in this channel. Moreover, Table II tells that there is $(1s)^3 ggg$ glueball state which can mix with the other states.

So we generalize the mixing matrix to the 4×4 matrix

$$M^2 = \begin{pmatrix} E + \frac{2}{3}\Delta & -\frac{\sqrt{2}}{3}\Delta & 0 & 0 \\ -\frac{\sqrt{2}}{3}\Delta & E + \frac{1}{3}\Delta + 3A & \nu & \nu' \\ 0 & \nu & G & \epsilon \\ 0 & \nu' & \epsilon & G' \end{pmatrix} \tag{41}$$

TABLE V. The numerical analysis of the mixing in the 2^{++} channel, with $f_2(1270)$ and $f_2(1950)$ as the input.

					$m_1 = f_2(1270)$			$m_2 = f_2(1950)$			m_3				
μ	A	ν	ζ	m_3	$u+d$	s	g	$u+d$	s	g	$u+d$	s	g	$R(m_2/m_1)$	$R(m_3/m_1)$
0.76	0.39	0.95	2.33	1.47	0.40	0.00	0.60	0.35	0.36	0.29	0.25	0.64	0.11	0.19	0.15
0.78	0.35	0.99	2.78	1.47	0.46	0.01	0.53	0.33	0.33	0.34	0.22	0.66	0.12	0.25	0.18
0.80	0.31	1.01	3.26	1.48	0.52	0.01	0.47	0.30	0.30	0.40	0.18	0.69	0.12	0.33	0.21
0.82	0.28	1.02	3.79	1.48	0.58	0.01	0.41	0.27	0.27	0.46	0.15	0.72	0.13	0.43	0.24
0.84	0.24	1.02	4.38	1.49	0.64	0.01	0.36	0.24	0.24	0.52	0.13	0.75	0.12	0.57	0.27
0.86	0.20	0.99	5.06	1.49	0.69	0.01	0.30	0.20	0.21	0.59	0.10	0.78	0.11	0.76	0.30

to include the ggg state. This has eight parameters, but we may express G and G' by the chromon mass μ and put $G = 4\mu^2$ and $G' = 9\mu^2$. This reduces the number of the parameters to seven.

Now, with

$$\begin{aligned} E &= \pi^2, \qquad \pi = \pi(140), \\ \Delta &= 2(K^2 - \pi^2), \qquad K = K(498), \end{aligned} \tag{42}$$

as the input we have to fix five more parameters. To do that we may impose the condition $\nu' = 3/2\nu$, because ν and ν' represent two and three gluon couplings to the isosinglet $q\bar{q}$. With this we can choose three physical states as the input and vary the chromon mass μ to predict the mass of the fourth physical state.

We could also try the condition $3A = \nu^2 + \nu'^2$, assuming

$$\begin{aligned} \langle q'\bar{q}'|H|q\bar{q}\rangle_{An} \simeq{}& \langle q'\bar{q}'|gg\rangle\langle gg|q\bar{q}\rangle \\ &+ \langle q'\bar{q}'|ggg\rangle\langle ggg|q\bar{q}\rangle. \end{aligned} \tag{43}$$

But again this constraint could be too stringent.

Now, if we choose $\eta'(958), \eta(1405)$ and $\eta(1760)$ as the input, we obtain Table VI. Notice that here we have two sets of solution, because the 4×4 mixing involves quadratic equation.

In this analysis the mass of the fourth physical state becomes around 550 MeV, which could be interpreted to be $\eta(548)$. The result shows that the physical contents of $\eta(1405)$ and $\eta(1760)$ depend very much on the mass of the gluon. On the other hand here $\eta(548)$ is a mixture of $u + d$ and s, but $\eta'(958)$ becomes predominantly a gg glue state. This is problematic and not in line with PDG, which interprets $\eta'(958)$ as predominantly a $q\bar{q}$ state.

Moreover, experimentally we have [17]

$$\begin{aligned} J/\Psi &\to \gamma\eta'(958) \simeq (5.15 \pm 0.16) \times 10^{-3}, \\ J/\Psi &\to \gamma\eta(548) \simeq (1.104 \pm 0.034) \times 10^{-3}, \end{aligned}$$

so that we expect

$$R(\eta(548)/\eta'(958)) \simeq 0.21 \pm 0.01. \tag{44}$$

But Table VI implies that this is very small

$$R(\eta(548)/\eta'(958)) \simeq 0.01. \tag{45}$$

This does not agree with PDG. This again is because the numerical analysis interprets $\eta'(958)$ to be predominantly a glue state.

We could choose different input. But with $\eta(548)$, $\eta'(958)$, and $\eta(1760)$ as the input we obtain very similar results. In this case the fourth physical state becomes $\eta(1405)$, and $\eta'(958)$ remains predominantly a two chromon bound state. So we have the same problem.

In this section we have discussed the numerical analysis of the quark gluon mixing in three channels 0^{++}, 2^{++}, and 0^{-+} below 2 GeV based on our quark and chromon model. Clearly the numerical result is inconclusive and should be viewed as preliminary.

In the 0^{++} and 2^{++} channels the numerical results seem to work, but in the 0^{-+} channel it has problem. On the other hand we emphasize that the above numerical analysis is not intended to provide a perfect mixing. Obviously it is a rough approximation which is expected to have uncertainty of at least 20 to 30%.

There are many reasons the above analysis cannot be perfect. First of all, the mixing discussed here neglected many things. For example, we have neglected the light

TABLE VI. The numerical analysis of the mixing in the 0^{-+} channel. Here we choose $\eta'(958)$, $\eta(1405)$, and $\eta(1760)$ as the input.

		$m_1 = \eta'(958)$				$m_2 = \eta(1405)$				$m_3 = \eta(1760)$				m_4			
μ	m_4	$u+d$	s	$2g$	$3g$	$u+d$	s	$2g$	$3g$	$u+d$	s	$2g$	$3g$	$u+d$	s	$2g$	$3g$
0.50	0.55	0.02	0.03	0.93	0.02	0.13	0.11	0.05	0.72	0.43	0.30	0.01	0.26	0.43	0.57	0.00	0.00
0.50	0.55	0.01	0.01	0.96	0.03	0.16	0.13	0.01	0.70	0.41	0.28	0.04	0.27	0.43	0.57	0.00	0.00
0.52	0.54	0.04	0.07	0.85	0.04	0.20	0.17	0.13	0.50	0.31	0.22	0.01	0.46	0.45	0.54	0.00	0.00
0.52	0.55	0.00	0.01	0.92	0.07	0.29	0.25	0.01	0.45	0.26	0.18	0.07	0.48	0.44	0.56	0.00	0.00
0.54	0.54	0.06	0.12	0.76	0.06	0.26	0.22	0.23	0.28	0.20	0.14	0.00	0.66	0.47	0.52	0.01	0.00
0.54	0.54	0.00	0.00	0.88	0.11	0.44	0.37	0.01	0.19	0.11	0.08	0.11	0.70	0.45	0.55	0.00	0.00

μ	m_4	$R(m_2/m_1)$	$R(m_3/m_1)$	$R(m_4/m_1)$	A	ν	ϵ
0.50	0.55	0.12	0.06	0.004	0.84	0.34	−0.07
0.50	0.55	0.46	0.13	0.003	0.84	0.30	0.28
0.52	0.54	0.03	0.08	0.006	0.75	0.40	−0.13
0.52	0.55	0.44	0.33	0.004	0.75	0.31	0.47
0.54	0.54	0.00	0.10	0.009	0.66	0.42	−0.20
0.54	0.54	0.26	0.64	0.003	0.66	0.24	0.64

hybrid $q\bar{q}g$ states which could influence the mixing very much. Moreover, the mixing depends on the input parameters, but there are many ways to choose the input. So we have to have a more thorough numerical analysis.

Nevertheless, our mixing analysis confirms the following. First, our quark and chromon model provides a conceptually simple way to identify the glueballs. Second, the mixing influences the physical contents of hadrons very much. This makes the mixing analysis more important.

An important outcome of the analysis is that the constituent mass of the chromon is around several hundred MeV. This seems to agree with the lattice result [13,14].

VI. HYBRIDS

The quark and chromon model predicts the hybrid hadrons made of quark and chromon. Clearly we can construct color singlet $q\bar{q}g$ mesons with one color octet chromon and a $q\bar{q}$ octet. Similarly we can have $qqqg$ baryons with one chromon and a qqq octet. So these hybrids must exist.

Of course, similar hybrid hadrons or multi-quark hadrons have also been proposed before [7,8]. But our model provides a unique picture of hybrid hadrons which is different from the other models of hybrids or multi-quark hadrons. In particular, it has unambiguous predictions and can in principle easily be distinguished from the other existing hybrids and/or multi-quark models.

To understand this, notice that on the surface our $q\bar{q}g$ hybrid mesons might look very similar to $qq\bar{q}\,\bar{q}$ states, because the chromon in $q\bar{q}g$ could be replaced by a $q\bar{q}$ octet. However, there is a clear difference between the tetra-quark states and our $q\bar{q}g$ hybrids. Obviously the $q\bar{q}$ forms octet and singlet, but our chromon has no singlet component. So the spectrum (i.e., the number of states) that they predict is different. In other words our hybrid model predicts less physical states.

Similarly our $qqqg$ hybrid baryons could be misidentified as $qqqq\bar{q}$ penta-quark states. But again the group theoretic structure of the two models is different. This confirms that the hybrids predicted by our quark and chromon model is different from other hybrids or multi-quark models. This means that by studying the spectrum we can tell which model is correct.

An important difference of these hybrids from the glueballs is that the hybrids have no intrinsic instability. This is because the chromon in $q\bar{q}g$ and $qqqg$ hadrons is stable, since there is no way that it can annihilate. So, unlike the glueballs, these hybrids are expected to have typical hadronic decay width.

What is really remarkable about our hybrid hadrons is that it is based on the quark and chromon model. It is a straightforward generalization of the quark model which comes from the existence of the valence gluons, and the physics behind it is as simple as the quark model. This simplicity translates to the clarity of the prediction. The predictions are straightforward and unambiguous. So we can easily qualify or disqualify the model experimentally. This is a most important feature of our hybrid model.

The remaining task is to identify the hybrid hadrons. Of course, PDG has already accumulated enough data which could be interpreted as hybrid hadrons and/or multi-quark hadrons. For example, there are quite many low-lying mesons which cannot be easily explained by the quark model, and some of them could be interpreted as a $q\bar{q}g$ hybrid. So we have to analyze these data carefully to find which model can correctly explain these data. This task will be tedious and time consuming, but certainly worthwhile to do.

The XYZ particles might be interesting candidates of the hybrids [57,58]. These particles have been interpreted as tetra-quarks mesons or meson-meson molecular bound states, but it would be worthwhile to see if they could also be understood as the $q\bar{q}g$ hybrids.

As we have remarked, the hybrid hadrons can influence the quarkonium-glueball mixing significantly. So understanding these hybrids is very important in the analysis of the mixing.

VII. MONOBALL: VACUUM FLUCTUATION OF MONOPOLE CONDENSATON

QCD generates the monopole condensation (more precisely the monopole-antimonopole pair condensation) which induces the dimensional transmutation and creates the mass gap. If so, one may ask what (if any) is the observable consequence of the monopole condensation. The answer could be the monoball.

To understand this, consider the ordinary superconductor in QED. It is well known that the Bardeen-Cooper-Schrieffer (BCS) superconductivity is characterized by two scales, the correlation length of the Cooper pair and the penetration length of the magnetic field. Field theoretically they are represented by two composite fields, a (complex) scalar field for the Cooper pair and a (massive) vector field for the confined magnetic field. And the existence of these modes are the consequence of the BCS superconductivity.

So in QCD we may expect a similar consequence of the monopole condensation. Naively we might think that the monopole condensation creates two mass scales, the correlation length of the monopole-antimonopole pairs and the penetration length of the chromo-electric flux. This suggests that the monopole condensation could induce two physical states, one 0^{++} and one 1^{++} vacuum fluctuation modes [20,21].

However, the confinement in QCD is not exactly dual to the superconductivity in QED. First of all, in QED the magnetic field to be confined is generated by the electric current, not by the magnetic charge. But in QCD the colored flux to be confined comes from the color charge, not the chromo-magnetic current. Second, in superconductor the Cooper pair has electric charge but the monopole-antimonopole pair in QCD obviously has no chromo-magnetic charge.

Third, in the superconductor the magnetic field is actually screened by the supercurrent, not confined by the Cooper pair. But in QCD the chromo-electric field is confined by the monopole-antimonopole pair. In other words, it is not the monopole supercurrent which provides the confinement. QCD has no monopole supercurrent. Fourth, the chromo-electric flux is described by the Coulomb (i.e., scalar) potential, not by the vector potential, in QCD. But in superconductor the magnetic field is described by the vector potential.

Finally, in the superconductor the Higgs mechanism takes place. The Landau-Ginzburg theory of superconductivity is a classic example of Higgs mechanism, where the spontaneous symmetry breaking generates the massive vector field which screens the magnetic field. But in QCD there is no spontaneous symmetry breaking. It is the dynamical symmetry breaking which generates the confinement. This tells us that the confinement mechanism in QCD is not exactly dual to the Meissner effect. They are different.

In particular, this implies that the penetration length in QCD could be represented by a scalar field, not by a spin-one field. This is because the chromo-electric field is described by the Coulomb (i.e., scalar) potential. This strongly suggests that both the correlation length and the penetration length in QCD must be represented by the scalar mode. In other words, there might be no 1^{++} vacuum fluctuation mode in QCD.

The remaining question is if the two scalar modes are different or not. In principle they could be different, but as we have shown in (22) the monopole condensation generates only one mass scale. This, together with the fact that QCD has only one scale $\Lambda_{\rm QCD}$, strongly suggests that they are the same.

From this we may conclude that the monopole condensation could have only one 0^{++} vacuum fluctuation mode which could naturally be called the magnetic glueball or simply the monoball. Clearly this fluctuation mode must be different from the glueballs made of the chromons because this characterizes the monopole condensation.

The importance of the monoball is that this represents the monopole condensation, so that the experimental verification of this monoball can be interpreted as the confirmation of the monopole condensation. This makes the experimental identification of the monoball a most urgent issue in QCD.

Ultimately, however, the nature of the monopole condensation (and the number of the vacuum fluctuation modes) should be determined by experiment, and it could well be that the monopole condensation has no vacuum fluctuation mode at all. To understand this possibility consider the Dirac sea, the vacuum of Dirac's theory of electron. It has vacuum bubbles made of electron-positron pairs, but is not the electron-positron pair condensation and apparently has no fluctuation mode.

So, if the QCD vacuum is like the Dirac sea, there will be no vacuum fluctuation and thus no monoball. At the moment it is not clear if the QCD vacuum is similar to Dirac sea, and only experiments can tell whether the nature of the QCD vacuum is different from the Dirac sea or not. This makes the experimental confirmation of the monoball more interesting.

One might ask if there is any candidate of the monoball. Actually PDG has several isoscalar 0^{++} states, in particular $f_0(500)$ and $f_0(980)$, which do not fit well in the quark model. It would be very interesting to find which of them (if at all) could be interpreted as the monoball.

Finally, it goes without saying that this vacuum fluctuation (if exists) could influence our analysis of the mixing in the 0^{++} channel. This is another complication we have to keep in mind in discussing the mixing.

VIII. DISCUSSIONS

In this paper we have discussed the hadron spectrum of the ECD obtained from the Abelian decomposition of QCD. Although ECD is mathematically identical to QCD, it makes the hidden dynamical structures of QCD explicit. In particular, it assures the existence of two types of gluons and generalizes the quark model to the quark and chromon model.

To compare this with other glueball models, consider the bag model which identifies the glueball as the colored field confined in a bag. In this picture the glueballs are made of infinite number of gluons in the form of the gluon field, so that there is no constituent gluon (i.e., a finite number of gluons) which make up the glueballs.

In contrast in the constituent model the glueballs are made of the constituent gluons. To bind the constituent gluons, however, we certainly need the binding gluons (i.e., the gluon field). Unfortunately this model does not tell us how to distinguish the binding gluons from the constituent gluons.

The Abelian decomposition tells us how to resolve this difficulty. It tells that there are indeed two types of gluons which play different roles, and naturally generalizes the quark model to the quark and chromon model. This provides a new picture of glueballs made of chromons. Moreover, this predicts new hybrid hadronic states which are made of quarks and chromons.

One of the main problems in hadron spectroscopy has been the identification of the glueballs. This identification is not simple for the following reasons. First, the glueballs have intrinsic instability which comes from the asymptotic freedom and antiscreening. Moreover, the glueballs in general may not exist as mass eigenstates because of the mixing with quarkoniums and other light hybrid mesons.

In this paper we have discussed how to identify them by discussing the glueball-quarkonium mixing in the numerical analysis. Clearly the mixing discussed here is a rough approximation, because it neglects the hybrids made of

$q\bar{q}g$ which could influence the mixing. Besides, the analysis depends on the input parameters, and there are many possibilities of choosing the input which we did not discuss in this paper. Nevertheless it tells us that the quark and chromon model provides a new picture of glueball-quarkonium mixing which can be easily tested by experiments.

In 0^{++} channel, our analysis is in line with (or at least not in contradiction with) PDG interpretation. It implies that $f_0(1500)$ could be predominantly the glue state. But here we must know which one, $a_0(980)$ or $a_0(1450)$, we should treat as the isotriplet partner of the isosinglet $q\bar{q}$ which mixes with the glueball. This is a very sensitive question, because the numerical analysis depends very much on this. PDG suggests $a_0(1450)$ to be the isotriplet partner. But this seems against the common sense, because $K_0^*(1430)$ made of $s\bar{s}$ becomes lighter than $a_0(1450)$. Clearly this issue remains to be settled.

Moreover, in this channel $f_0(500)$ and $f_0(980)$ have been puzzling [17]. For example, $f_0(500)$ has unusually broad width, and has been the subject of a large number of theoretical works. It has been suggested to be a tetra-quark state or $K\bar{K}$ molecules [44,45,59,60]. Unfortunately our analysis does not reveal much about their content.

In 2^{++} channel our analysis could explain the physical content of $f_2(1270)$, $f_2{}'(1525)$, and $f_2(1950)$ quite well. In particular it could predict the relative ratio of the Ψ radiative decay. This is remarkable. But we have to keep in mind that there are many other so-called unconfirmed physical states below 2 GeV in this channel, and they have to be studied more carefully.

Finally in 0^{-+} channel, our mixing analysis was problematic. It implies that $\eta'(958)$ is predominantly two glue state, but this view is against the PDG suggestion. On the other hand, it is well known that this channel has a long history of problems, and even the origin of the octet-singlet mixing in this channel has not been completely understood yet. Moreover, the existence of a light glueball made of three chromons makes the situation worse. So it is natural that our mixing analysis is least successful. To clarify these complications we certainly need a more thorough analysis.

Independent of the details, however, we emphasize the conceptual simplicity and clarity of the quark and chromon model. ECD makes QCD simple by decomposing it to the restricted part which describes the core dynamics of QCD and the valence part which represents the colored source of QCD. This provides the clear picture of the glueballs and hybrid hadrons. Moreover, this provides a clear picture of the glueball-quarkonium mixing.

In particular, ECD allows us to demonstrate the monopole condensation, more precisely the monopole-antimonopole pair condensation [25,26]. In this paper we have discussed how to verify this monopole condensation experimentally by searching for the monoball, the 0^{++} vacuum fluctuation of the monopole condensation.

The monoball, if exist, could have mass around $\Lambda_{\rm QCD}$. This implies that $f_0(500)$ could be the monoball candidate. Of course, at the moment it is not clear if this is the case. But the search for the monoball should be treated as one of the most important issue in QCD, because this could confirm the monopole condensation in QCD.

The main purpose of this paper was to provide the general framework of the glueball-quarkonium mixing mechanism. We hope to provide a more complete numerical mixing analysis in a separate publication [61].

ACKNOWLEDGMENTS

The work is supported in part by the National Natural Science Foundation of China (Grants No. 11175215, No. 11447105, and No. 11475227), Chinese Academy of Sciences Visiting Professorship for Senior International Scientists (Grant No. 2013T2J0010), Basic Science Research Program through the National Research Foundation of Korea (NRF) funded by the Ministry of Science and Future Planning (Grant No. 2012-002-134), and by Konkuk University.

TABLE VII. Suggested $q\bar{q}$ quark model interpretation of the light meson states from PDG. In the table the classification of the 0^{++} mesons is supposed to be tentative.

		I = 1	I = $\frac{1}{2}$	I = 0	I = 0	I = 0	I = 0
$1\ ^{2s+1}l_J$	J^{PC}	$u\bar{d}, \bar{u}d, (d\bar{d}-u\bar{u})/\sqrt{2}$	$u\bar{s}, d\bar{s}, \bar{d}s, \bar{u}s$	f'	f	$c\bar{c}$	$b\bar{b}$
$1\ ^1S_0$	0^{-+}	π	K	$\eta(548)$	$\eta'(958)$	$\eta_c(2984)$	$\eta_b(9398)$
$1\ ^3S_1$	1^{--}	$\rho(770)$	$K^*(892)$	$\phi(1020)$	$\omega(782)$	$J/\psi(3097)$	$\Upsilon(9460)$
$1\ ^1P_1$	1^{+-}	$b_1(1235)$	$K_{1B}{}^\dagger$	$h_1(1380)$	$h_1(1170)$	$h_c(3525)$	$h_b(9899)$
$1\ ^3P_0$	0^{++}	$a_0(1450)$	$K_0^*(1430)$	$f_0(1710)$	$f_0(1370)$	$\chi_{c0}(3415)$	$\chi_{b0}(9859)$
$1\ ^3P_1$	1^{++}	$a_1(1260)$	$K_{1A}{}^\dagger$	$f_1(1420)$	$f_1(1285)$	$\chi_{c1}(3511)$	$\chi_{b1}(9893)$
$1\ ^3P_2$	2^{++}	$a_2(1320)$	$K_2^*(1430)$	$f_2{}'(1525)$	$f_2(1270)$	$\chi_{c2}(3556)$	$\chi_{b2}(9912)$
$1\ ^1D_2$	2^{-+}	$\pi_2(1670)$	$K_2(1770)^\dagger$	$\eta_2(1870)$	$\eta_2(1645)$		
$1\ ^3D_1$	1^{--}	$\rho(1700)$	$K^*(1680)$		$\omega(1650)$	$\psi(3770)$	
$1\ ^3D_2$	2^{--}		$K_2(1820)$				
$1\ ^3D_3$	3^{--}	$\rho_3(1690)$	$K_3^*(1780)$	$\phi_3(1850)$	$\omega_3(1670)$		
$2\ ^3S_1$	1^{--}	$\rho(1450)$	$K^*(1410)$	$\phi(1680)$	$\omega(1420)$		

APPENDIX: ADDITIONAL INFORMATION

In the Appendix we summarize some useful data for our analysis in Tables VII and VIII from the Particle Data Group Review.

TABLE VIII. Low-lying isosinglet mesons which do not fit easily in the quark model listed by PDG.

States	J^{PC}	Mass (MeV)	Width (MeV)	Decay modes	Branch ratio (%)
$f_0(500)$	0^{++}	$400 \sim 550$	$400 \sim 700$	$\pi\pi$	dominant
				$\gamma\gamma$	seen
$f_0(980)$	0^{++}	990 ± 20	$40 \sim 100$	$\pi\pi$	dominant
				$K\bar{K}, \gamma\gamma$	seen
$\eta(1295)$	0^{-+}	1294 ± 4	55 ± 5	$\eta\pi\pi, a_0(980)\pi$	seen
$\eta(1405)$	0^{-+}	1409 ± 2	51 ± 3	$K\bar{K}\pi, \eta\pi\pi$	seen
				$a_0(980)\pi, 4\pi, \rho\rho$	seen
$\omega(1420)$	1^{--}	$1400 \sim 1450$	$180 - 250$	$\rho\pi$	dominant
				$\omega\pi\pi$	seen
$\eta(1475)$	0^{-+}	1476 ± 4	85 ± 9	$K\bar{K}\pi$	dominant
				$a_0(980)\pi, \gamma\gamma$	seen
$f_0(1500)$	0^{++}	1505 ± 6	109 ± 7	$\pi\pi$	34.9 ± 2.3
				4π	49.5 ± 3.3
				$K\bar{K}$	8.6 ± 1.0
				$\eta\eta$	5.1 ± 0.9
				$\eta\eta'(958)$	1.9 ± 0.8
$\eta_2(1645)$	2^{-+}	1617 ± 5	181 ± 11	$a_0(980)\pi, a_2(1320)\pi, K^*\bar{K}$	seen
				$K\bar{K}\pi, \eta\pi^+\pi^-$	seen
$\phi(1680)$	1^{--}	1680 ± 20	150 ± 50	$K\bar{K}^*(892)$	dominant
				$k\bar{K}, e^+e^-$	seen
$f_2(1950)$	2^{++}	1944 ± 12	472 ± 18	$K\bar{K}, K^*(892)\bar{K}^*(892)$	seen
				$\pi\pi, 4\pi, \eta\eta, \gamma\gamma$	seen

[1] H. Fritzsch and P. Minkowski, Nuovo Cimento **30A**, 393 (1975).
[2] P. G. O. Freund and Y. Nambu, Phys. Rev. Lett. **34**, 1645 (1975).
[3] J. Kogut, D. Sinclair, and L. Susskind, Nucl. Phys. **B114**, 199 (1976).
[4] R. L. Jaffe and K. Johnson, Phys. Lett. **60B**, 201(1976).
[5] P. Roy and T. Walsh, Phys. Lett. **78B**, 62 (1978).
[6] J. Coyne, P. Fishbane, and S. Meshkov, Phys. Lett **91B**, 259 (1980).
[7] M. Chanowitz, Phys. Rev. Lett. **46**, 981 (1981).
[8] K. Ishikawa, Phys. Rev. Lett. **46**, 978 (1981).
[9] J. Cornwall and A. Soni, Phys. Lett. **120B**, 431 (1983).
[10] C. Amsler and N. Tornqvist, Phys. Rep. **389**, 61 (2004).
[11] V. Mathieu, N. Kochelev, and V. Vento, Int. J. Mod. Phys. E **18**, 1 (2009).
[12] W. Ochs, J. Phys. G, **40**, 043001 (2013).
[13] G. S. Bali, K. Schilling, A. Hulsebos, A. C. Irving, C. Michael, and P. W. Stephenson, Phys. Lett. B **309**, 378 (1993).
[14] C. Morningstar and M. Peardon, Phys. Rev. D **60**, 034509 (1999).
[15] W. Lee and D. Weingarten, Phys. Rev. D **61**, 014015 (1999).
[16] Y. Chen *et al.*, Phys. Rev. D **73**, 014516 (2006).
[17] K. Olive *et al.* (Particle Data Group), Rev. Part. Phys., Chin. Phys. C **38**, 090001 (2014).
[18] J. Dudek *et al.*, Eur. Phys. J. A **48**, 187 (2012).
[19] Y. M. Cho, Phys. Rev. D **21**, 1080 (1980).
[20] Y. M. Cho, Phys. Rev. Lett. **46**, 302 (1981).
[21] Y. M. Cho, Phys. Rev. D **23**, 2415 (1981).
[22] W. S. Bae, Y. M. Cho, and S. W. Kimm, Phys. Rev. D **65**, 025005 (2001).
[23] Y. S. Duan and M. L. Ge, Scientia Sinica **11**,1072 (1979).
[24] Y. M. Cho and S. H. Ie, Proc. Coll. Nat. Sci. **14**, 27 (1989).
[25] Y. M. Cho, Franklin H. Cho, and J. H. Yoon, Phys. Rev. D **87**, 085025 (2013).
[26] Y. M. Cho, Int. J. Mod. Phys. A **29**, 1450013 (2014).
[27] Y. M. Cho, Phys. Rev. D **62**, 074009 (2000).
[28] G. 't Hooft, Nucl. Phys. **B190**, 455 (1981).
[29] S. Kato, K. Kondo, T. Murakami, A. Shibata, T. Shinohara, and S. Ito, Phys. Lett. B **632**, 326 (2006).
[30] S. Ito, S. Kato, K. Kondo, T. Murakami, A. Shibata, and T. Shinohara, Phys. Lett. B **645**, 67 (2007).
[31] N. Cundy, Y. M. Cho, W. Lee, and J. Leem, Phys. Lett. B **729**, 192 (2014).

[32] N. Cundy, Y. M. Cho, W. Lee, and J. Leem, Nucl. Phys. **B895**, 64 (2015).
[33] V. Schanbacher, Phys. Rev. D **26**, 489 (1982).
[34] Y. M. Cho and D. G. Pak, Phys. Rev. D **65**, 074027 (2002).
[35] Y. M. Cho, M. L. Walker, and D. G. Pak, J. High Energy Phys. 05 (2004) 073.
[36] J. Schwinger, Phys. Rev. **82**, 664 (1951).
[37] Y. M. Cho and D. G. Pak, Phys. Rev. Lett. **86**, 1947 (2001); **91**, 039101 (2003).
[38] D. Gross and F. Wilczek, Phys. Rev. Lett. **30**, 1343 (1973).
[39] H. Politzer, Phys. Rev. Lett. **30**, 1346 (1973).
[40] T. Barnes and F. Close, Phys. Lett. **116B**, 365 (1982).
[41] N. Isgur and J. Paton, Phys. Rev. D **31**, 2910 (1985).
[42] P. Lacock, C. Michael, P. Boyle, and P. Rowland, Phys. Lett. B **401**, 308 (1997).
[43] C. Bernard, T. Burch, E. B. Gregory, D. Toussaint, C. DeTar, J. Osborn, S. Gottlieb, U. M. Heller, and R. Sugar, Phys. Rev. D **68**, 074505 (2003).
[44] R. L. Jaffe, Phys. Rev. D **15**, 267 (1977).
[45] J. Weinstein and N. Isgur, Phys. Rev. D **41**, 2236 (1990).
[46] D. Morgan and M. Pennington, Phys. Rev. D **48**, 1185 (1993).
[47] L. Faddeev and A. Niemi, Phys. Rev. Lett. **82**, 1624 (1999).
[48] S. Shabanov, Phys. Lett. B **458**, 322 (1999); **463**, 263 (1999).
[49] H. Gies, Phys. Rev. D **63**, 125023 (2001).
[50] R. Zucchini, Int. J. Geom. Methods Mod. Phys. **01**, 813 (2004).
[51] Y. M. Cho, Phys. Rev. Lett. **44**, 1115 (1980).
[52] B. de Witt, Phys. Rev. **162**, 1195 (1967); **162**, 1239 (1967).
[53] W. S. Bae, Y. M. Cho, and D. G. Pak, Phys. Rev. D **64**, 017303 (2001).
[54] See for example, M. Peskin and D. Schroeder, *An Introduction to Quantum Field Theory* (Addison-Wesley, Reading, MA, 1995); S. Weinberg, *Quantum Theory of Fields* (Cambridge University Press, Cambridge, England, 1996).
[55] C. Amsler and F. Close, Phys. Rev. D **53**, 295 (1996).
[56] F. Close and A. Kirk, Eur. Phys. J. C **21**, 531 (2001).
[57] S. L. Zhu, Phys. Lett. B **625**, 212 (2005).
[58] F. E. Close and P. R. Page, Phys. Lett. B **628**, 215 (2005).
[59] J. Oller, E. Oset, and J. Pelaez, Phys. Rev. Lett. **80**, 3452 (1998).
[60] A. G Nicola and J. Pelaez, Phys. Rev. D **65**, 054009 (2002).
[61] P. Zhang, J.-J. Xie, Li-Ping Zou, and Y. M. Cho (to be published).